Research Report

Journal of INTERNATIONAL MEDICAL RESEARCH

Journal of International Medical Research
2016, Vol. 44(1) 54–66

DOI: 10.1177/0300060515600186
imr.sagepub.com
SAGE

Application of spectral computed tomography dual-substance separation technology for diagnosing left ventricular thrombus

Hong Zeng[1], Meng-Chao Zhang[2], Yu-Quan He[1], Lin Liu[2], Ya-Liang Tong[1] and Ping Yang[1]

Abstract

Objective: To investigate the value of spectral computed tomography (CT) dual-substance separation technology for diagnosing left ventricular (LV) thrombus.

Methods: In this observational case–control study, spectral CT scans were conducted in patients with and without LV thrombi. Densities in the regions of the LV cavity, papillary muscles and LV thrombus were observed on 140kVp mixed-energy and 70 keV single-energy images. Iodine and blood were chosen as the base material pair, the densities were observed and the iodine and blood concentrations were quantitatively measured.

Results: A total of 24 patients were enrolled in this study. On iodine-based density images, both the LV thrombus and papillary muscles showed low-attenuation shadows. On blood-based density images, comparable high-density attenuation was found in the LV thrombus and LV cavity, while relative hypodensity was noted in the papillary muscles. Iodine and blood densities were significantly lower in papillary muscles than in the LV cavity. Iodine densities were significantly lower in the LV thrombus than the LV cavity, whereas blood densities in the two areas did not differ significantly.

Conclusions: Spectral CT dual-substance separation technology and its derived images of iodine- and blood- based densities provide a new, simple, and feasible semiquantitative method to detect LV thrombus that warrants further investigation.

Keywords

Thrombosis, left ventricle, tomography, X-radiography computer, spectral imaging

Date received: 13 March 2015; revised: 14 July 2015; accepted: 20 July 2015

[1]Division of Cardiology, China-Japan Union Hospital of Jilin University, Changchun, Jilin Province, China
[2]Division of Radiology, China-Japan Union Hospital of Jilin University, Changchun, Jilin Province, China

Corresponding author:
Ping Yang, Division of Cardiology, China-Japan Union Hospital of Jilin University, 126 Xiantai Street, Changchun, Jilin Province, China 130033.
Email: pyang@jlu.edu.cn

Introduction

Left ventricular (LV) thrombosis is often accompanied by peripheral vascular thromboembolic complications such as ischaemic stroke, thus has a high morbidity and mortality.[1–3] Timely and effective anticoagulative/antithrombotic therapy could reduce (or even completely dissolve) the thrombi. Therefore, the accurate detection of the LV thrombus is essential for clinicians to determine treatment strategies and to improve the patient's prognosis. Currently, two-dimensional transthoracic echocardiography (TTE) is the most commonly used technique for detecting LV thrombi.[4,5] It provides information such as shape, size and anatomical site of the thrombus, but occasionally trabecular muscles, false chordae tendineae and papillary muscle tumours may be misdiagnosed as thrombi. Magnetic resonance imaging (MRI) has been validated as a fairly accurate modality to diagnose LV thrombi.[6,7] However, it is not suitable for all patients due to increased contraindications, higher cost and slower imaging speed compared with TTE. Spectral computed tomography (CT) imaging, a newly developed technology, has been applied in areas such as coronary artery imaging,[8] plaque recognition[9,10] and myocardial perfusion,[11] but no data have been reported on its application in the identification of LV thrombi.

The aim of this study was to investigate the use of a gemstone spectral imaging (GSI) CT scanner to identify LV thrombi using CT spectra based on their unique dual-substance separation technology and derived single substance isolated images.

Patients and methods

Patients

Patients who underwent coronary CT angiography in the Division of Cardiology, China-Japan Union Hospital of Jilin University, Changchun, Jilin Province, China between December 2013 and March 2014 were enrolled sequentially into this observational case–control study. All patients underwent a TTE examination within 3 days prior to CT examination. On the basis of the TTE results, patients were divided into two groups: group 1 consisted of patients who had no cardiac thrombus; group 2 consisted of patients with LV thrombus detected by TTE, and the diagnosis was further confirmed with sequential TTE follow-ups with regular antithrombotic therapy using warfarin. Patients in groups 1 and 2 were age and sex matched. Ethical approval was obtained from the Ethics Committee of the China-Japan Union Hospital of Jilin University (No. 20140338). Written informed consent was obtained from the patients prior to their inclusion in the study.

TTE examination

Two-dimensional TTE examinations were performed using a Philips Sonos® 5500 colour Doppler ultrasound system (Philips Healthcare, Best, the Netherlands) and standard techniques, in accordance with the guidelines of the American Society of Echocardiography.[12] LV thrombus was defined as an echodense mass within the LV cavity with margins distinct from the LV wall, visible in both systole and diastole in at least two views, with a morphology that was different from tissues such as papillary muscles, chordae tendineae, trabecular muscles or technical artefacts. TTE results were reviewed by two experienced ultrasonography examiners.

Spectral CT scan

A Discovery CT750 HD scanning system (GE Healthcare, Milwaukee, WI, USA) was used in the GSI mode. All patients signed an additional informed consent form prior to undergoing their CT angiography examination. The patient's heart rate was

controlled at <70 beats/min, and each patient lay in a supine position, connected to an electrocardiogram (ECG) and a binocular high-pressure injector. The positioning line was set at 1–2 cm below the trachea carina to cardiac diaphragm surface. Contrast agent application was controlled by the bolus tracking technique. A total of 20 ml nonionic iodinated contrast media iohexl (Omnipaque™ 350 mg/ml; GE Healthcare) was injected via the cubital vein with a velocity of 5 ml/s, followed by 15 ml saline injected at the same velocity. A region of interest (ROI) was placed into the aortic root, and image acquisition began 6 s after the density level reached the predefined threshold of 100 Hounsfield units. The patient was then instructed to hold his/her breath, and a further 70–80 ml of contrast media was infused intravenously at the same velocity followed by 30–40 ml of saline. Scanning parameters were as follows: X-radiography tube helical scan speed, 0.6 s/cycle; pitch, 0.969; detector width, 4 cm; instantaneous voltage switch (0.5 ms) between high and low energy (140 kVp and 80 kVp); and tube current, 600 mA. Two modes were selected for image reconstruction: the first set of images was reconstructed using 140 kVp mixed energy; the second set of images was constructed using 70 keV single energy. The reconstructed slice thickness and slice spacing was 2.50 mm.

Image analysis and measurement

Image analysis and measurement in group 1 patients. Reconstructed images using 140 kVp mixed energy and 70 keV single energy were transferred to a GE Advantage Workstation 4.6 (GE Healthcare). Image densities in the regions of the normal LV cavity and papillary muscles were visually observed. In the GSI viewer software, iodine and blood were chosen as the base material pair. Then, in the generated isolated images of iodine- and blood-based density, the densities in the regions of the normal LV cavity and papillary muscles were simultaneously compared with visual observations. Subsequently, a scanning slice showing the clearest images and maximum papillary muscles was selected, and a ROI with a size of 3 mm × 3 mm was set in the regions of the papillary muscles and within the normal LV cavity for the same slice, respectively. Iodine and blood densities at these ROIs were qualitatively measured, based on the respective isolated images of iodine- and blood-based density. Five ROIs were set for each slice in the LV cavity and papillary muscles, respectively, and the measurements were repeated in three different slices. The mean results were used for statistical analysis.

Image analysis and measurement in group 2 patients. Using the aforementioned method for patients without thrombi, densities were observed in the normal LV cavities and thrombi on the mixed-energy 140 kVp and single-energy 70 keV images. The identification of an LV thrombus was made by two attending radiologists (M.C.Z. and L.L.) with reference to the TTE images. Simultaneous comparative observations of densities in the regions of the LV cavity and thrombus on the isolated images of iodine- and blood-based density were made; the mean iodine and blood densities in the regions of the normal LV cavity and thrombi were qualitatively measured.

According to the obtained observations and analysis results, retrospective analyses, slice by slice, were undertaken of the isolated images of the iodine- and blood-based density in the patients with LV thrombus. On the basis of the different manifestations of LV papillary muscles and thrombus on spectral CT, normal papillary muscles and LV thrombotic lesions were identified when they coexisted at the same scanning slice.

Cardiac MRI scans (MAGNETOM® Skyra 3.0 T scanner; Siemens Healthcare,

Erlangen, Germany) were conducted in patients with idiopathic hypereosinophilic syndromes associated with LV thrombi. Cine MRI was performed with breath holding, retrospective ECG-gating and true fast imaging with steady-state precession sequence.

All patients diagnosed with an LV thrombus received 40 mg (equivalent of 4000 IU anti-Xa activity) of low-molecular weight heparin sodium (Clexane®; Aventis Intercontinental, Antony, France) subcutaneously twice daily and 2.5–5.0 mg of warfarin (Xiinyi Jiufu Pharmaceutical Co., Shanghai, China) orally once daily for 3–5 days. Following discharge from hospital, patients continued to receive 2.5–9.0 mg of warfarin orally once daily for at least 1 month; the dose of warfarin was adjusted according to an INR of 2.0–3.0. TTE was rechecked at 1 month after initial treatment.

Statistical analyses

SigmaSTAT® 3.5 software (Systat Software, San Jose, CA, USA) was used for statistical analyses. Data were expressed as mean ± SD for continuous variables with normal distribution. Data were expressed as median (25th–75th percentile) for continuous variables without a normal distribution. Student's *t*-tests were performed in order to compare continuous variables with normal distribution. The paired-sample *t*-test was used to compare blood and iodine densities between the LV cavity and thrombus and between the LV cavity and papillary muscles for the same slice. An independent-samples *t*-test was used to compare differences in the blood and iodine densities of the LV thrombus and papillary muscles between the two groups. Nonparametric Mann–Whitney *U*-test was used to compare samples with a not-normal distribution. A P-value < 0.05 was considered statistically significant.

Results

Twenty-four patients who underwent coronary CT angiography, including 16 male and eight female patients (age range, 26–79 years; mean ± SD age, 56.3 ± 16.5 years), were enrolled in the study. On the basis of the TTE results, patients were divided into two groups. Group 1 consisted of 12 patients who had no cardiac thrombus (eight male and four female; age range 30–78 years; mean age ± SD, 56.4 ± 15.9 years), including two patients with acute myocardial infarction (AMI) within 2 weeks of onset, four patients with chronic myocardial infarction (>3 month onset of AMI), four patients with dilated cardiomyopathy and two patients with atrial fibrillation before radiofrequency ablation. Group 2 consisted of 12 patients (eight male and four female; age range 26–79 years; mean age ± SD, 56.1 ± 17.7 years) with LV thrombus detected by TTE. The diagnosis was further confirmed with sequential TTE follow-ups with regular antithrombotic therapy using warfarin. Two patients had AMI within 2 weeks of onset, four patients had chronic myocardial infarction, four patients had dilatated cardiomyopathy and two patients had idiopathic hypereosinophilic syndromes. A single thrombus was detected in nine patients and two or more thrombi in three patients, on TTE. Thrombi varied in size among patients with the maximum being 41.2 mm × 27.8 mm and the minimum being 10.5 mm × 7.4 mm on TTE. Two patients with idiopathic hypereosinophilic syndromes underwent cardiac MRI examination.

In group 1 patients on iodine-based density images, the LV cavity with normal filling of contrast agent manifested as a high-density attenuation, while papillary muscles appeared as low-density attenuation or filling defects (Figure 1A). On the blood-based density images, the density of the papillary muscles was relatively lower compared with the LV cavity with visual

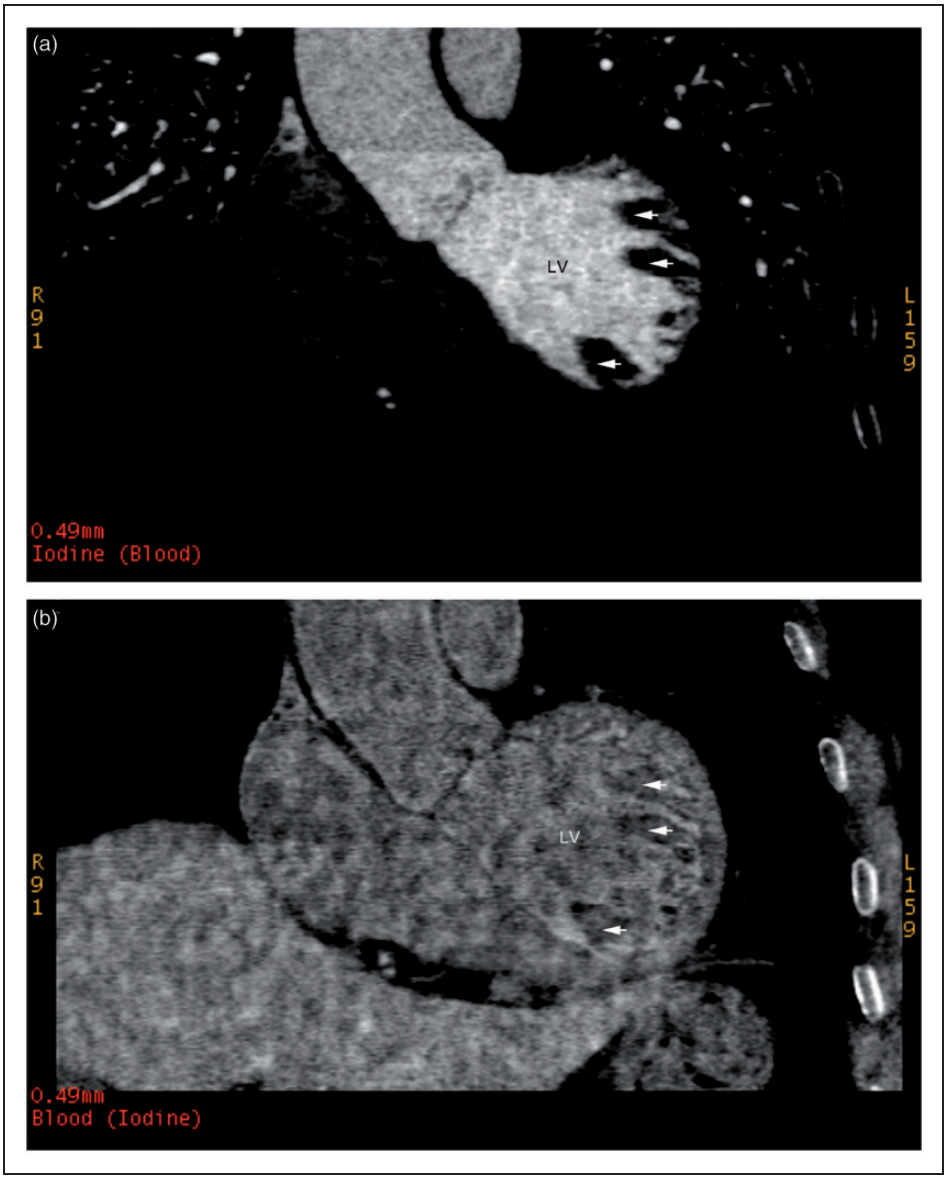

Figure 1. Representative contrast-enhanced iodine- and blood-based density images in a patient without a cardiac thrombus from group 1: (a) an iodine (blood)-based density image; and (b) a blood (iodine)-based density image (arrows indicate the papillary muscle regions). LV, left ventricle.

observations (Figure 1B). Quantitative iodine and blood concentrations in the papillary muscles were significantly lower than those in the LV cavities ($P < 0.001$; Table 1).

In group 2 patients on iodine-based density images, the LV cavity with normal filling of contrast agent manifested as high-density attenuation, while the LV thrombus appeared as low-density attenuation or

Table 1. Comparison of iodine and blood densities for the normal left ventricular (LV) cavity, papillary muscles and LV thrombus in patients with or without LV thrombi who underwent coronary imaging with spectral computed tomography dual-substance separation technology.

	Group 1		Group 2	
Parameter	LV cavity $n = 12$	Papillary muscles $n = 12$	LV cavity $n = 12$	LV thrombus $n = 12$
Blood density, mg/cm^3	1068.40 ± 10.78	1022.31 ± 14.38[a]	1063.08 ± 7.63	1057.73 ± 10.06
Iodine density, mg/cm^3	18.27 ± 3.97	4.23 ± 1.54[a]	17.13 ± 3.45	1.75 ± 1.07[a]
Blood density difference	–	44.99 (38.81–56.63)	–	2.88 (1.23–5.95)[b]
Iodine density difference	–	13.64 ± 2.13	–	12.30 ± 1.21

Data presented as mean ± SD or median (25th–75th percentile).
[a]Versus respective LV cavity, $P < 0.001$ (paired-sample *t*-test); [b]LV thrombus versus papillary muscles, $P < 0.001$ (nonparametric Mann–Whitney *U*-test).

filling defects (Figure 2A). On the blood-based density images, density in the LV thrombotic region was relatively high and comparable with the normal LV cavity with visual observations (Figure 2B). The mean iodine concentration in the LV thrombus was significantly lower than that in the normal LV cavity ($P < 0.001$), while no difference was found in the mean blood concentrations between these areas (Table 1).

In the 12 patients without cardiac thrombus in group 1, the mean iodine and blood densities in papillary muscles were subtracted from those in the LV cavity at the same slice, to obtain the iodine and blood density differences between papillary muscles and the LV cavity for each slice. This process was repeated in three different scanning slices, and the mean value was used for each patient's final iodine and blood density differences between papillary muscles and the LV cavity. Using the same method, iodine and blood density differences were obtained between the LV thrombus and LV cavity in the 12 patients with LV thrombus in group 2. Statistical analyses showed that the iodine density difference in the LV thrombus was similar to that in papillary muscles, while the blood density difference was significant between these two areas ($P < 0.001$; Table 1).

On the basis of the results described above, slice by slice, the isolated iodine- and blood-density images were simultaneously analysed in patients with LV thrombus in group 2. For each patient, it was possible to easily and clearly identify LV thrombotic lesions from normal papillary muscles. Figure 3 illustrates the CT spectrum images for a patient who had mixed papillary muscles and LV thrombus in the same slice. On the iodine-based density image, both papillary muscles and LV thrombus presented with less filling of contrast agent. On the blood-based density image, the papillary muscles showed a relatively lower density, while the LV thrombus showed a density similar to the LV cavity. Therefore, the differentiation between the papillary muscles and the LV thrombotic lesion could be made by the simultaneous observation of the images of the iodine and blood densities in the same slice. The measured iodine and blood concentrations confirmed the visual observation results (Figure 3).

In this study, two patients with LV thrombus underwent cardiac MRI scans. The single cine MRI images showed low-density signals in the regions of the LV thrombus for both patients (Figure 4). All patients in group 2 received low-molecular

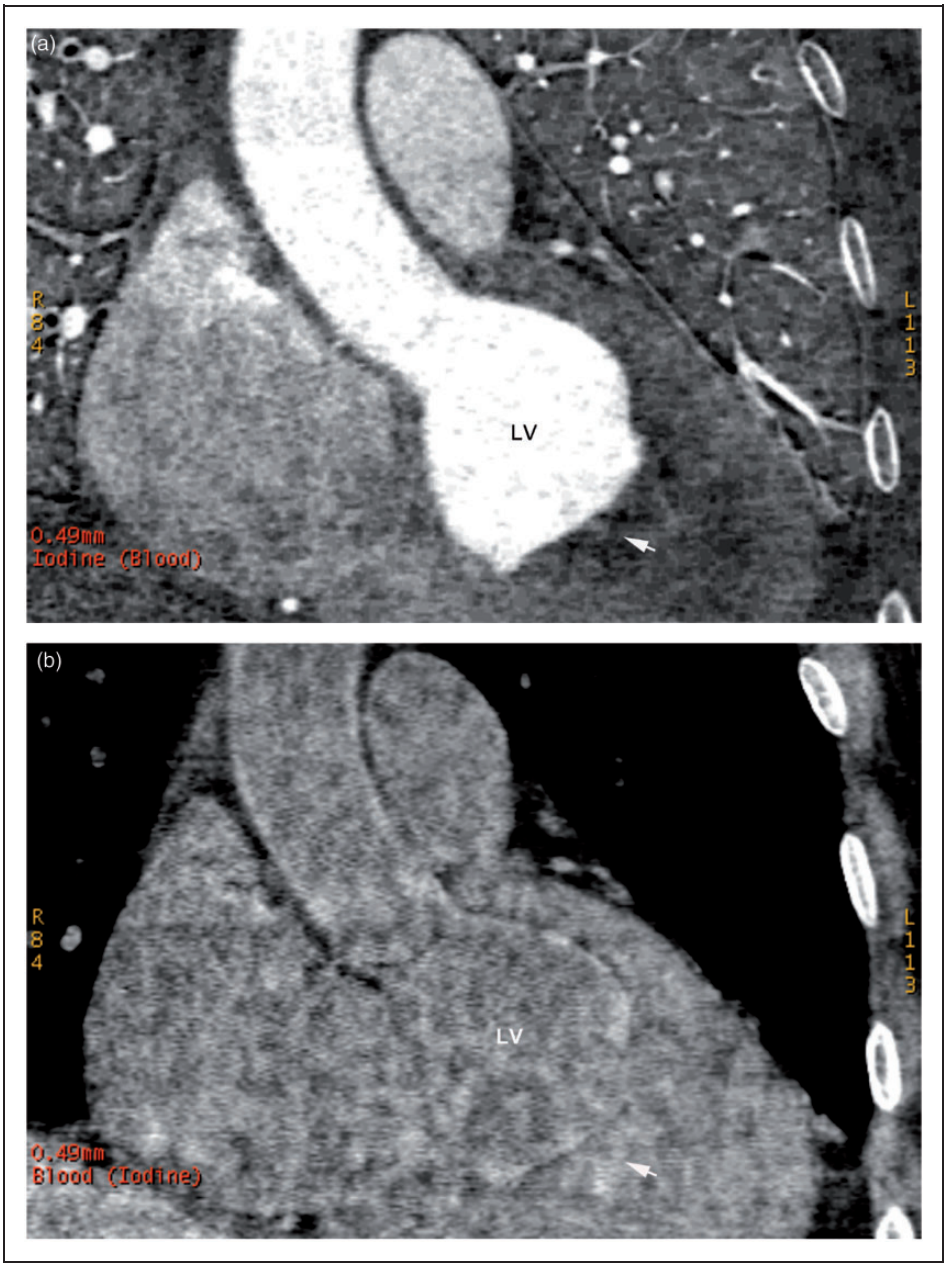

Figure 2. Representative contrast-enhanced iodine- and blood-based density images in a patient with a left ventricular thrombus from group 2: (a) an iodine (blood)-based density image; and (b) a blood (iodine)-based density image (arrows indicate the thrombotic regions). LV, left ventricle.

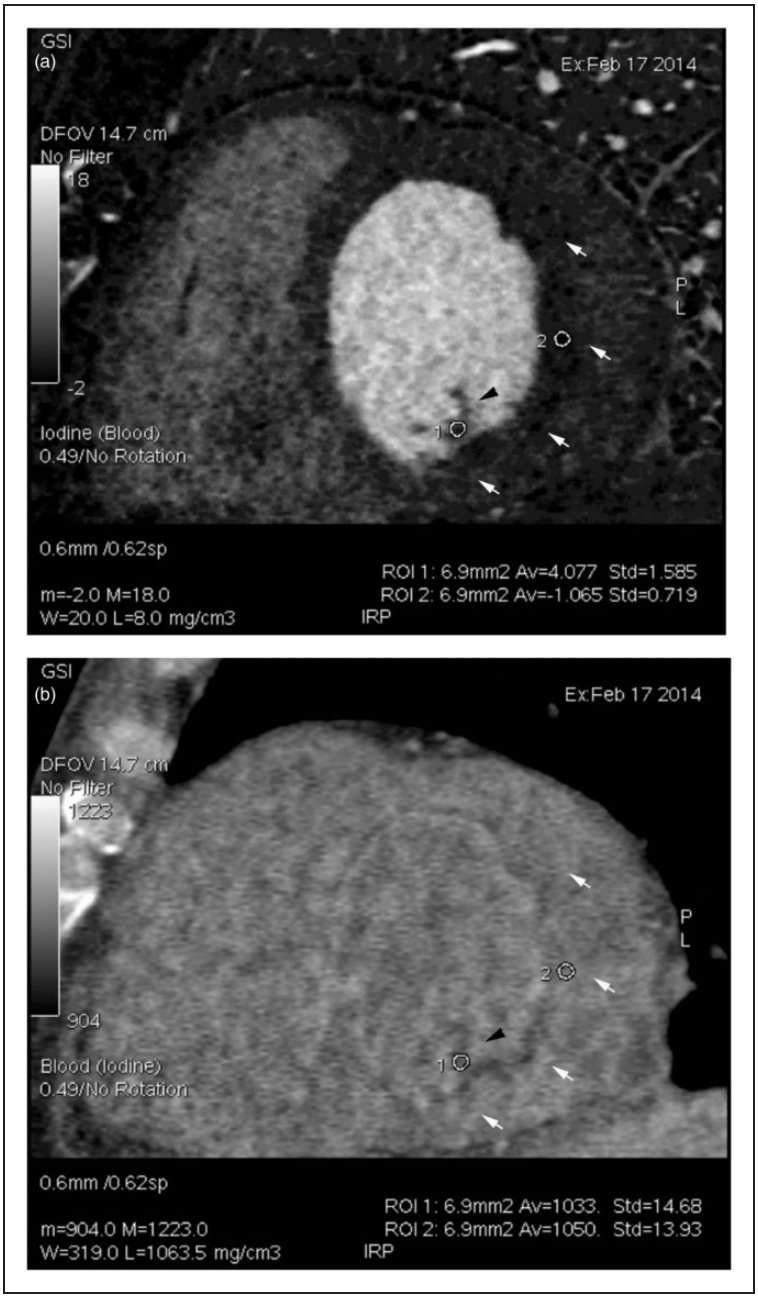

Figure 3. Representative contrast-enhanced iodine- and blood-based density images in a patient with a left ventricular (LV) thrombus from group 2: (a) an iodine (blood)-based density image; and (b) a blood (iodine)-based density image. Numbers 1 and 2 indicate regions of interest (ROIs) in the regions of the papillary muscles and LV thrombus, respectively. White arrows indicate the contour of the thrombus, and the black arrow indicates the papillary muscle region. Densities of iodine and blood at the ROIs are shown at the right bottom of the images: iodine density, papillary muscle 4.077 ± 1.585 mg/cm^3, LV thrombus 1.065 ± 0.719 mg/cm^3; blood density, papillary muscle 1033 ± 14.68 mg/cm^3, LV thrombus 1050 ± 13.93 mg/cm^3.

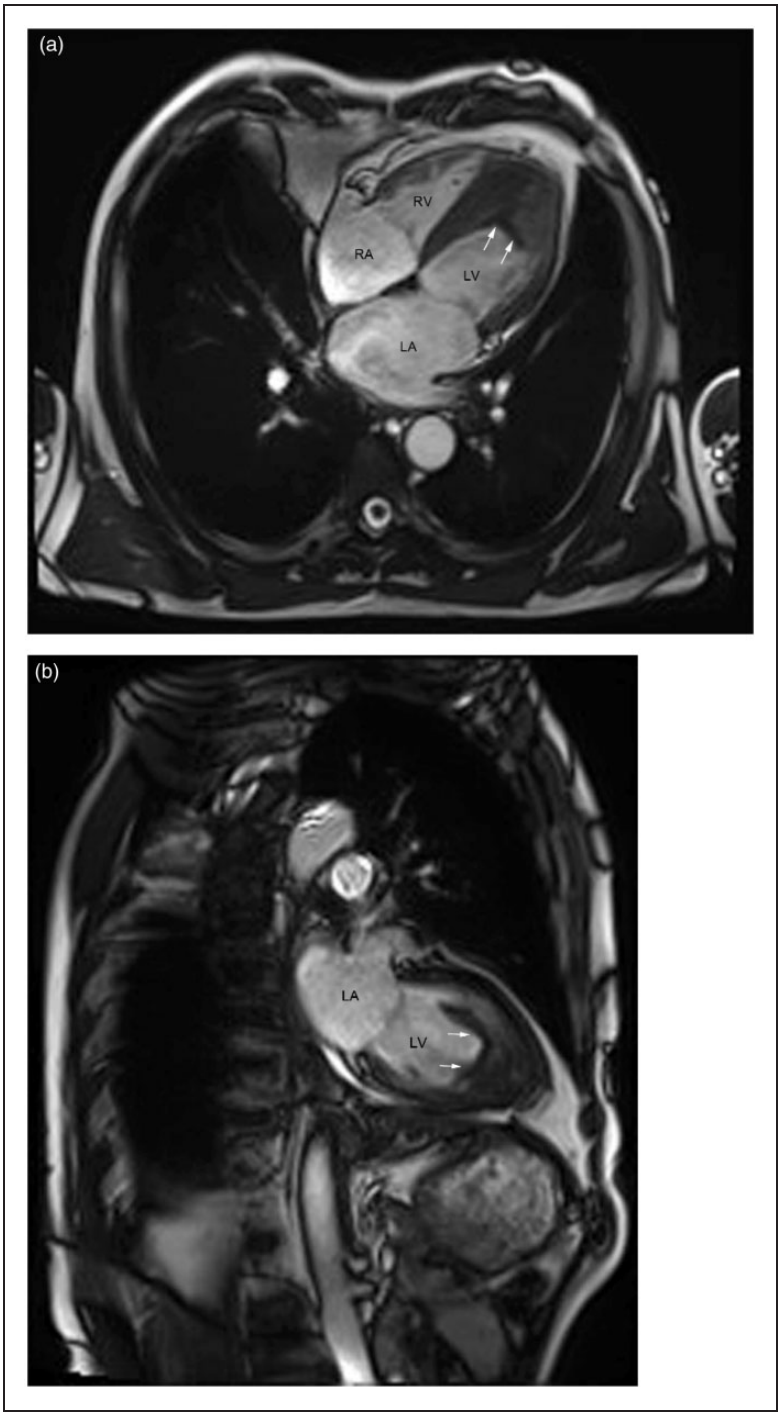

Figure 4. Representative single cine magnetic resonance images undertaken using true fast imaging with steady-state precession sequence in one patient with idiopathic hypereosinophilic syndrome: (a) left ventricle (LV) four-chamber long axis plane; (b) LV two-chamber long axis plane. White arrows indicate the borders of the thrombus. Scan parameters: repetition time = 40 ms, echo time = 1.4 ms, layer thickness = 6 mm, field of view = 340 mm × 340 mm, reversal angle = 57°. RV, right ventricle; RA, right atrium; LA, left atrium.

weight heparin and warfarin therapy. One month later, TTE follow-up results revealed an obvious shrinkage in the size of the LV thrombi in 11 patients (data not shown).

Discussion

Left ventricular thrombosis is common in patients with AMI, ventricular aneurysm[13] and dilated cardiomyopathy.[1] Occasionally, LV thrombus can be found in patients with hypertrophic cardiomyopathy and hypereosinophilia.[14,15] It is often accompanied by peripheral vascular thromboembolic complications such as stroke, and thus has a high mortality and morbidity.[2–3,13] LV thrombi may be significantly reduced or even completely dissolved if timely and effective anticoagulant and/or antithrombotic therapy is administered.[16] Therefore, timely and accurate detection of LV thrombi is essential in order to develop treatment strategies and improve the patient's prognosis.

Currently, TTE has been proposed as the most commonly used standard modality for detecting LV thrombi.[4,5] However, a large variation exists in the results obtained by different operators, and up to 46% of cardiac thrombi diagnosed with TTE are uncertain.[4,5] Occasionally, structures such as trabecular muscles, false chordae tendinae and papillary muscle tumours may be misdiagnosed as LV thrombi.[6] Cardiac MRI has been validated as a fairly accurate modality to detect cardiac thrombi,[6,7] but due to its higher cost, more contraindications, lower imaging speed and longer examination time compared with TTE, it is not appropriate for all patients. Multislice spiral CT (MSCT) angiography is a widely accepted method for the evaluation of coronary arteries. While clearly revealing the three-dimensional coronary arteries, MSCT is capable of showing the low-density shadows or filling defects caused by thrombotic lesions. However, conventional nonspectral MSCT cannot be used to make a qualitative diagnosis based on tissue composition or accurately identify thrombotic lesions from normal papillary muscles. This is because papillary muscles are also manifest as low-density shadows on routine CT images.

The present study showed that spectral CT dual-substance separation technology using a GSI scanner and its derived iodine- and blood-based density images allow the simple and clear identification of LV thrombi. To our knowledge, this is the first report to describe the use of this new spectral CT imaging technique for this purpose.

Compared with conventional MSCT, spectral CT imaging is a newly developed technology.[17] It utilizes a single X-radiography tube and an instantaneous switching between high and low voltage of 80 kVp and 140 kVp within 0.5 ms to obtain two sets of X-radiography sampling data almost simultaneously, for the same layer and in the same direction. In addition to generating 101 single-energy images,[18] it can decompose the attenuation coefficient of one substance into a weighted sum of any other two substances (base material pair), thereby achieving composition analysis and substance separation.[19]

Using spectral CT dual-substance separation technology and selecting blood and iodine as the base material pair, the isolated images of iodine (blood)-based and blood (iodine)-based density were obtained. On iodine-based density images, both normal papillary muscles and LV thrombi appeared as low-density shadows, which represented a reduced filling by contrast medium. On blood-based density images, densities and measured blood concentrations in LV thrombi were similar to the normal LV cavity, while lower densities and quantitative blood concentrations were noted in papillary muscles. Thus, by simultaneously comparing the blood- and iodine-based images for the same slice, LV thrombotic lesions could be easily differentiated from normal papillary muscles. This spectral CT

capability cannot be achieved with the traditional MSCT method.

Normal papillary muscles and LV thrombi have different manifestations on isolated blood- and iodine-based density images, which may be closely related to their different material composition and blood supply characteristics. Iodine is the main component of CT-enhanced contrast agent, and the iodine-based density images show the contrast agent (iodine) distribution, therefore reflecting the tissue's blood supply.[20] It is more difficult for the contrast agent (iodine) to reach the regions of the papillary muscles and LV thrombus, compared with the normal LV cavity. Thus, these areas exhibited a lower iodine density compared with the LV cavity on the isolated iodine-based density images. In contrast, since the LV thrombus is a condensed mass with blood components coagulated within the LV cavity, its composition is similar to the blood components in the LV cavity (both contain platelets and erythrocytes). Therefore, the observed densities and the measured blood concentrations are similar for the LV thrombus and the normal LV cavity. Conversely, papillary muscle composition includes fibrous tissue and smooth muscle, which is quite different from blood or clot components in the LV cavity and thrombus. Therefore, observed densities and quantitative blood concentrations in papillary muscles are different from the normal LV cavity and thrombotic lesions on the isolated blood-based density images.

This study also demonstrated that the LV thrombi could be reduced if a timely and accurate anticoagulant and/or antithrombotic therapy, such as low-molecular weight heparin sodium and warfarin, were administered.

In addition to cardiac thrombi, cardiac-occupying lesions include primary cardiac tumours, cardiac metastases and infective valvular vegetation. Spectral CT dual-substance separation technology may provide a new method to identify cardiac-occupying lesions such as tumours. The blood supply characteristics of cardiac thrombus and tumours are different. Kirkpatrick et al.[21] adopted contrast-enhanced ultrasound perfusion and found no contrast-enhanced phenomenon in cardiac thrombi due to a lack of blood supply. Using this feature, it should be easy to differentiate between cardiac thrombi and tumours. Since the composition of cardiac tumours is different from clots and blood within the cardiac lumen, it is anticipated that simultaneous comparative analysis of the isolated blood- and iodine-based density images on spectral CT for the same slice will be helpful for differentiating cardiac thrombotic lesions from tumours. This hypothesis needs to be validated through future clinical investigations.

This present study had a number of limitations. First, the sample size was small so these current findings should be interpreted as a 'proof of principle', which demonstrates the feasibility of this new method for assessing cardiac thrombi. Future studies with larger sample sizes in which the investigators are blind to the TTE results are warranted to validate the present observational findings; and to determine the sensitivity, specificity, positive predictive value, and negative predictive value of this new technique. Secondly, TTE examination was used as the gold standard for the detection of LV thrombi, but histopathological confirmation were not performed. Thirdly, no validation or discrimination among diseases such as cardiac tumours was undertaken, and no atrium/left atrial appendage thrombi were investigated in this study. It should be noted that the current application of spectral CT is still in its initial stages, therefore more clinical experience and validation is required.

In conclusion, spectral CT dual-substance separation technology and the derived images of blood- and iodine-based

density allow the semiquantitative identification of the tissue components of LV thrombi. This technology provides a new, simple, and feasible method for detecting LV thrombotic lesions, and may provide a new method for identifying other LV-occupying lesions such as cardiac tumours. Further validation with larger clinical samples is warranted.

Acknowledgment

The authors would like to thank two ultrasonography experts Dong-Mei Gao, MD PhD and Jun Song, MD PhD at the Ultrasonography Department from our hospital for their involvement.

Declaration of conflicting interests

The authors declare that there are no conflicts of interest.

Funding

This study was supported by a research grant from Health and Family Planning Commission of Jilin Province, China (No: 2014Z063).

References

1. Stokman PJ, Nandra CS and Asinger RW. Left ventricular thrombus. *Curr Treat Options Cardiovasc Med* 2001; 3: 515–521.
2. Falk RH, Foster E and Coats MH. Ventricular thrombi and thromboembolism in dilated cardiomyopathy: a prospective follow-up study. *Am Heart J* 1992; 123: 136–142.
3. Stratton JR and Resnick AD. Increased embolic risk in patients with left ventricular thrombi. *Circulation* 1987; 75: 1004–1011.
4. Saranteas T, Alevizou A, Tzoufi M, et al. Transthoracic echocardiography for the diagnosis of left ventricular thrombosis in the postoperative care unit. *Crit Care* 2011; 15: R54.
5. Thanigaraj S, Schechtman KB and Perez JE. Improved echocardiographic delineation of left ventricular thrombus with the use of intravenous second-generation contrast image enhancement. *J Am Soc Echocardiogr* 1999; 12: 1022–1026.
6. Srichai MB, Junor C, Rodriguez LL, et al. Clinical, imaging, and pathological characteristics of left ventricular thrombus: a comparison of contrast-enhanced magnetic resonance imaging, transthoracic echocardiography and transesophageal echocardiography with surgical or pathological validation. *Am Heart J* 2006; 152: 75–84.
7. Weinsaft JW, Kim HW, Crowley AL, et al. LV thrombus detection by routine echocardiography: insights into performance characteristics using delayed enhancement CMR. *JACC Cardiovasc Imaging* 2011; 4: 702–712.
8. Fuchs TA, Stehli J, Fiechter M, et al. First experience with monochromatic coronary computed tomography angiography from a 64-slice CT scanner with Gemstone Spectral Imaging (GSI). *J Cardiovasc Comput Tomogr* 2013; 7: 25–31.
9. Baturin P, Alivov Y and Molloi S. Spectral CT imaging of vulnerable plaque with two independent biomarkers. *Phys Med Biol* 2012; 57: 4117–4138.
10. Zainon R, Ronaldson JP, Janmale T, et al. Spectral CT of carotid atherosclerotic plaque: comparison with histology. *Eur Radiol* 2012; 22: 2581–2588.
11. Pang LF, Zhang H and Lu W. Spectral CT imaging of myocardial infarction: preliminary animal experience. *Eur Radiol* 2013; 23: 133–138.
12. Schiller NB, Shah PM, Crawford M, et al. Recommendations for quantitation of the left ventricle by two-dimensional echocardiography. American Society of Echocardiography Committee on Standards, Subcommittee on Quantitation of Two-Dimensional Echocardiograms. *J Am Soc Echocardiogr* 1989; 2: 358–367.
13. Delewi R, Zijlstra F and Piek JJ. Left ventricular thrombus formation after acute myocardial infarction. *Heart* 2012; 98: 1743–1749.
14. Holloway CJ, Betts TR, Neubauer S, et al. Hypertrophic cardiomyopathy complicated by large apical aneurysm and thrombus, presenting as ventricular tachycardia. *J Am Coll Cardiol* 2010; 56: 1961.

15. Buyuktas D, Eskazan AE, Borekci S, et al. Hypereosinophilic syndrome associated with simultaneous intracardiac thrombi, cerebral thromboembolism and pulmonary embolism. *Intern Med* 2012; 51: 309–313.
16. Cregler LL. Antithrombotic therapy in left ventricular thrombosis and systemic embolism. *Am Heart J* 1992; 123(4 Pt 2): 1110–1114.
17. Pessis E, Campagna R, Sverzut JM, et al. Virtual monochromatic spectral imaging with fast kilovoltage switching: reduction of metal artifacts at CT. *Radiographics* 2013; 33: 573–583.
18. Matsumoto K, Jinzaki M, Tanami Y, et al. Virtual monochromatic spectral imaging with fast kilovoltage switching: improved image quality as compared with that obtained with conventional 120-kVp CT. *Radiology* 2011; 259: 257–262.
19. Lv P, Zhang Y, Liu J, et al. Material decomposition images generated from spectral CT: detectability of urinary calculi and influencing factors. *Acad Radiol* 2014; 21: 79–85.
20. Zhang XF, Lu Q, Wu LM, et al. Quantitative iodine-based material decomposition images with spectral CT imaging for differentiating prostatic carcinoma from benign prostatic hyperplasia. *Acad Radiol* 2013; 20: 947–956.
21. Kirkpatrick JN, Wong T, Bednarz JE, et al. Differential diagnosis of cardiac masses using contrast echocardiographic perfusion imaging. *J Am Coll Cardiol* 2004; 43: 1412–1419.